Journal of Power Sources 438 (2019) 227059

Contents lists available at ScienceDirect

Journal of Power Sources

journal homepage: www.elsevier.com/locate/jpowsour

Activation-free synthesis of microporous carbon from polyvinylidene fluoride as host materials for lithium-selenium batteries

Mohammad Hossein Aboonasr Shiraz [a], Hongzheng Zhu [a], Yulong Liu [b], Xueliang Sun [b], Jian Liu [a,*]

[a] School of Engineering, Faculty of Applied Science, University of British Columbia, Kelowna, BC, V1V 1V7, Canada
[b] Department of Mechanical and Materials, University of Western Ontario, London, ON, N6A 5B9, Canada

HIGHLIGHTS

- One-step activation-free synthesis of microporous carbon (MPC) from PVDF.
- MPC/Se showed high excellent performance as cathode in Li-Se batteries.
- Properties of MPC/Se depend on pore size and volume, and Se content in MPC/Se.
- Micropores and micropore volume are the key merits for porous carbon as the Se host.

GRAPHICAL ABSTRACT

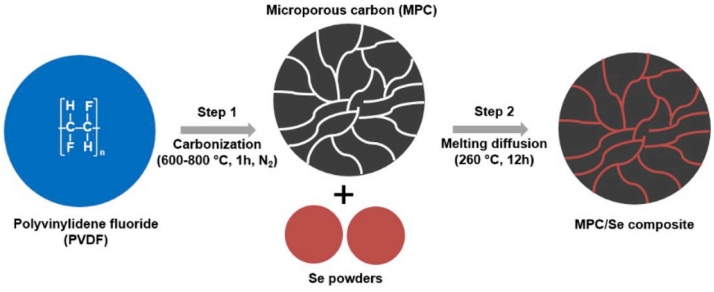

ARTICLE INFO

Keywords:
Lithium–selenium battery
Carbonate-based electrolyte
Microporous carbon
Polyselenides

ABSTRACT

Microporous carbon (MPC) was synthesized from polyvinylidene fluoride (PVDF) using an activation-free approach and used as a selenium host for high-performance lithium-selenium (Li-Se) batteries. The microporous carbon/selenium (MPC/Se) composites were applied a cathode in Li-Se batteries with a carbonate-based electrolyte. The influences of PVDF carbonization temperature (600 °C, 700 °C and 800 °C) and Se content (50 wt%, 60 wt%, and 70 wt%) in the cathode were investigated in order to establish correlation between MPC structure and MPC/Se electrochemical performance. The results revealed that the MPC/Se composite cathode, with MPC synthesized at 800 °C and with a Se content of 50 wt%, exhibited a superior reversible capacity of 508.8 mAh g^{-1} at 0.1C after 100 cycles. Moreover, the MPC/Se maintained a capacity retention of 354.0 mAh g^{-1} at 0.5C for 200 cycles. The reason for the excellent performance could be attributed to the dominant microporous feature of MPC, which could effectively confine Se and reduce side reactions with electrolytes. Furthermore, increasing Se content from 50 wt% to 70 wt% leaded to decrease in the specific capacity and rate capability of MPC/Se cathode, due to significantly reduced Li-ion diffusion coefficient. This work suggested the effectiveness of MPC derived from commercial PVDF through an activation-free and scalable approach as Se hosts for high-performance Li-Se batteries.

* Corresponding author.
E-mail address: jian.liu@ubc.ca (J. Liu).

https://doi.org/10.1016/j.jpowsour.2019.227059
Received 13 June 2019; Received in revised form 12 August 2019; Accepted 21 August 2019
Available online 24 August 2019

1. Introduction

Nowadays, energy storage is one of the top-rated concerns in order to increase the deployment of renewable energy globally, decrease the dependence on fossil fuels, and reduce greenhouse gas emissions. Lithium-ion batteries are the most popularly used energy storage technology for many applications, such as electric vehicles, portable devices, and grid storage, due to their relatively high energy density and low cost [1]. However, the fast-growing demands from end users calls for battery technologies with higher capacity, longer lifetime and lower cost. Lithium-ion batteries are reaching the bottleneck of their performance, due to the limitation in the battery chemistry, and cannot satisfy these increasing requirements [2,3]. Recently, lithium-sulfur (Li–S) batteries have drawn great attentions owing to their high theoretical energy density of 2570 Wh kg^{-1} and the low cost of S [4,5]. Despite of considerable progresses made over the past years, Li-S batteries still face many challenges associated with the insulating nature of S and "shuttle effect" phenomena, which results from the dissolution of high-order polysulfide intermediates in ether-based electrolytes [6,7]. Therefore, it is urgent to develop alternatives to S cathode in order to enable high-performance lithium-based batteries.

Recently, elemental selenium (Se) has attracted increasing attentions as a promising cathode material to build lithium-selenium (Li-Se) batteries. Se is a *d*-electron-containing member in the same elemental group as S in the periodic table, and has a considerably higher electronic conductivity of 1×10^{-3} S m^{-1} than S (5×10^{-28} S m^{-1}) [8–10]. The reaction of Se with Li follows the reaction of $2Li^+ + Se + 2e^- \leftrightarrow Li_2Se$, corresponding to a gravimetric capacity of 675 mAh g^{-1}, which is much lower than that of S (1672 mAh g^{-1}) [8–10]. However, Se possesses a high density of 4.2 g cm^{-3}, and provides a high theoretical volumetric capacity of 5253 mAh cm^{-3}, comparable to that of S (3467 mAh cm^{-3}) [9]. Since the first report by Amine and co-authors in 2012 [10], these advantages of Se in electronic conductivity and volumetric energy density have motivated researchers to explore the possibility of using Se as a cathode for Li-Se batteries.

Earlier work employed bulk Se or nanostructured Se cathodes in ether-based electrolytes in Li-Se batteries [11–13]. Similar as S cathodes, Se cathodes exhibited severe shuttle effect, limited life cycle, and Coulombic efficiency in ether-based electrolytes, due to highly reactive high-order polyselenides (Li_2Se_x, $x > 4$). Later on, it was reported that polyselenides were insoluble in carbonate-based electrolytes [14]. As a result, Se cathode, especially space-confined Se, were more compatible with carbonate-based electrolytes, and showed high capacity and outstanding cycling stability [16–24]. In carbonate-based electrolytes, Se undergoes a one-step reaction from Se to Li_2Se, without the formation of unstable polyselenide intermediates, and is featured with one single plateau in its charge-discharge curves [8,9]. Therefore, development of Li-Se batteries based on carbonate-based electrolytes represents a promising approach to develop alternatives to LIBs and Li-S batteries.

Rational design of Se cathode is the key to enabling high-capacity and durable Li-Se batteries. In particular, confining Se in porous carbon matrix has been proven as an effective approach to enable high-performance Se cathode for Li-Se batteries. In recent work, various porous carbon materials have been developed as Se hosts to improve the overall performance of Li-Se batteries, including hierarchical porous carbon derived from metal organic framework (MOF) or zeolitic imidazolate framework (ZIF) [16–18], nitrogen-doped microporous carbon [19,20], and porous carbon spheres [21–24]. For instance, Guo et al. prepared a ordered mesoporous carbon (CMK-3) matrix as a Se host and demonstrated a high discharge capacity of 670 mAh g^{-1} at 0.1C for the Se/CMK-3 cathode [24]. In another work, by using ZIF-derived microporous carbon and novel electrolyte additives (LiDFOB and FEC), Wang et al. achieved a capacity of 511 mAh g^{-1} for 1000 cycles at 5C, with a capacity decay of 0.012% per cycle for the nanostructured Se cathode [16]. Despite of these great progresses in Se cathode design, synthesis of porous carbon materials used in these work involved complex processes and/or expensive precursors (as summarized in Tables SI–1), making them difficult to scale up for practical applications. For example, although ZIF-8 derived carbon nanoparticles (~35 nm) promised fast kinetics and good rate capability for Se cathode, the preparation of these carbon nanoparticles consisted of several steps, *i.e.* synthesis of ZIF-8, followed by carbonization at high temperatures and then washing with a HCl solution [16,17]. In another two studies, polyacrylonitrile nanofibers [15] and polypyrrole spheres [19] were first synthesized, then carbonized, and finally chemically activated using KOH, followed with a washing process. Furthermore, the majority of Se cathodes reported so far have relatively low Se loading (<1 mg cm^{-2}) and Se content (<50 wt%) [16–25]. Se loading represents the mass of Se per unit electrode area, while Se content stands for the weight percentage of Se in the Se/C composites. Ideally, both Se loading and Se content should reach as high as possible in order to achieve high energy density in Li-Se batteries at the battery system level [26,27]. To address the aforementioned limitations, therefore, it is imperative to develop an easy, scalable, and low-cost fabrication approach for porous carbon material with preferably high Se loading and Se content in Se/C cathode composites for Li-Se batteries.

Herein, we developed a one-step activation-free process to fabricate microporous carbon (MPC) as Se hosts for Li-Se batteries based on a carbonate electrolyte. This work has thee highlights as follows. First of all, MPC with a high surface area (830.0 m^2 g^{-1}) and dominant micropores (1–3 nm) was prepared by direct pyrolysis of commercial polyvinylidene fluoride (PVDF) powders in one step and used for Se infiltration without any further activation. The MPC synthesis method is easy to scale up at relatively low cost. Secondly, the optimal MPC/Se composite cathode showed a high reversible specific capacity of 530 mAh g^{-1} and high Coulombic efficiency (CE) over 99.5% at 0.1C, and maintained a capacity of 400 mAh g^{-1} at 0.5C for 200 cycles with a high Se loading of 1.4 mg cm^{-2}. At finally yet importantly, this work established the correlations between the physical properties of MPC, Se loadings and Se contents, and electrochemical properties of MPC/Se cathode, and pinpointed the key factors governing the performance of Li-Se batteries in carbonate-based electrolytes.

2. Experimental

2.1. Preparation of MPC and MPC/Se composites

Poly (vinylidene fluoride) (PVDF, $(–CH_2CF_2–)_n$, MW: 64.035 g mol^{-1}, Alfa Aesar) was used as the starting material without further purification. Microporous carbon (MPC) was obtained by direct pyrolysis of PVDF at high temperatures (600, 700 and 800 °C) for 1 h under a nitrogen (99.999%) environment. The pyrolysis was performed in a tube furnace (Lindberg/Blue M Mini-Mite) with a heating rate of 10 °C min^{-1}. Black products collected after pyrolysis were MPC, and no further activation on MPC was required. It should be noted that since decomposition of PVDF released corrosive hydrogen fluoride (HF) gas, stainless steel tube was used to hold PVDF and calcium carbonate aqueous solution was used to neutralize exhausted gas from the tube furnace. From this point forward, the MPC pyrolyzed at 600, 700 and 800 °C was denoted as MPC-600, MPC-700 and MPC-800, respectively.

MPC and Se composites (MPC/Se) were prepared by a melting diffusion method [23]. Briefly, MPC and Se powders (99.5%, Sigma Aldrich) were firstly mixed in different weight ratios (50:50, 40:60, and 30:70) in a mortar for 1 h. Secondly, the MPC and Se mixture was sealed in a 50 mL stainless-steel autoclave under an argon (99.999%) environment. Lastly, the autoclave was heated to 260 °C and hold for 12 h to facilitate the diffusion of Se into microspores of MPC, as a result of capillary forces. The obtained MPC/Se composites with nominal Se loadings of 50 wt%, 60 wt%, and 70 wt% were designated as MPC-X/Se 50, MPC-X/Se 60, and MPC-X/Se 70, respectively, where X equals to 600, 700 and 800 (carbonization temperatures). The actual Se loadings in the MPC/Se composites were measured by thermogravimetric

analysis (TGA, NETZSCH STA 449F3).

2.2. Structural characterization of MPC and MPC/Se composites

The morphologies and structure of MPC and MPC/Se composites were characterized by using a scanning electron microscope (SEM) equipped with energy-dispersive X-ray spectroscopy (EDS) (Tescan MIRA3), a high resolution transmission electron microscopy (HRTEM, JEOL 2010F), and a powder X-ray diffraction system (XRD, Bruker D8 Advance, Cu K_α X-ray source). TG analysis was conducted on MPC/Se composites in NETZSCH STA 449F3 in a nitrogen atmosphere from room temperature (RT) to 900 °C at a rate of xx °C min^{-1}. Raman spectra were recorded on a HORIBA Scientific LabRAM HR Raman spectrometer system equipped with a 532.4 nm laser. The isotherms of N_2 gas adsorption on the samples were collected at 77 K using TriStar II 3020 surface area analyzer.

2.3. Electrochemical characterizations of MPC/Se composites

The electrochemical properties of the MPC/Se composites were evaluated in CR 2032 coin cells by using Li foil as the counter electrode. To prepare the cathode electrode, 80 wt% of MPC/Se composite, 10 wt% of carbon black (MTI), and 10 wt% of sodium alginate (Ward's Science Co., Ltd., 0.5 wt% aqueous solution) were mixed thoroughly to form a uniform slurry. The slurry was then pasted on an aluminum foil using a doctor blade. The electrode was completely dried at 50 °C under vacuum overnight. After that, the electrode was cut into round disks with a diameter of 12.7 mm and Se loadings in a range of 1.4–2.0 mg cm^{-2}. Coin cells were assembled in an argon (99.999%) filled glovebox workstation with H_2O and O_2 level below 0.1 ppm. One coin cell consisted of one Se/C electrode as the cathode, one Li metal as the anode, Celgard 2500 as the separator. The electrolyte used is 1 M $LiPF_6$ in ethylene carbonate:diethyl carbonate (EC:DEC, 1:1 vol ratio). The cycling performance of the coin cells was tested in the voltage range of 1–3 V (or 0.5 – 3 V) on a Neware BTS 4000 battery testing system. Cyclic voltammetry (CV) testing was performed on a Biologic VSP Potentiostat/Galvanostat Station in the voltage range of 1–3 V (*vs.* Li^+/Li) at a scan rate of 0.2 mV s^{-1}. The electrochemical testing was conducted at room temperature of 25 °C. The specific capacity was calculated based on the Se loading weight in each MPC/Se composite.

3. Results and discussion

Fig. 1 illustrates the preparation process for microporous carbon (MPC) and MPC/Se composites. The MPC is synthesized from one-step carbonization of PVDF at temperatures of 600–800 °C in a N_2 environment for 1 h. In the first step, thermal decomposition of PVDF leads to the formation of micropores in MPC structure, and is accompanied with the release of corrosive HF gas [28,29]. In the second step, MPC was mixed with Se powders in various weight ratios (50:50, 40:60, and 30:70), and the mixture was annealed at 260 °C for 12 h to infiltrate Se into the pores of MPC to form MPC/Se composites.

Fig. 2 shows the morphology and structure of MPC and MPC/Se composites. The obtained MPC possesses irregular shapes with particle sizes of about 10–100 μm, as seen in Fig. 2a. High-resolution transmission electron microscopy (HRTEM) observation discloses the presence of short-range ordered carbon layers and many micropores less than 3 nm imbedded in the structure of MPC, as pointed by the white arrows in Fig. 2b. Fig. 2c presents BET isotherms and pore size distribution of MPC carbonized at 800 °C (MPC-800). MPC-800 exhibits type I isotherm with the significant feature of "microporous solids" [28,29]. The knee of adsorption took place at a very low pressure and the plateau is fairly flat, indicating a strong interaction between pore walls and adsorbate, as a feature of highly microporous carbon [28,29]. The insert in Fig. 2c shows the pore size distribution of MPC-800, which exhibits a narrow single modal pore size distribution between 1 and 3 nm in the micropore region. MPC-700 and MPC-600 possess similar features in BET isotherms, as will be discussed later on. Compared to MPC, MPC/Se composites show no obvious morphology change (Fig. 2d). EDS elemental mapping under Scanning Transmission Electron Microscopy (STEM) mode confirms the existence of C and Se (Figure SI-1), and the uniform distribution of Se in MPC carbon structure, as seen in Fig. 2e. X-ray diffraction (XRD) patterns of pristine Se, MPC-800, and MPC-800 with a Se content of 50% (MPC-800/Se 50) are shown in Fig. 2f. It can be seen that pure Se powders exhibit sharp and intense peaks. Diffraction peaks of pure Se are located at 23.5°, 29.7°, 41.3°, 43.7°, 45.4°, 51.7°, 56.1°, 61.7°, 65.2°, corresponding to (100), (101), (110), (012), (111), (201), (112), (022), (120) planes of trigonal Se (JCPDS No: 06-0362), respectively. For MPC-800, only one broad peak is detected in its XRD pattern, suggesting the amorphous nature of MPC carbon, which is in agreement with HRTEM in Fig. 2b. For MPC-800/Se 50, all the characteristic diffraction peaks related to pure Se disappear, and on one broad peak is found located at about 25°, implying all Se are buried into the micropores of MPC. TGA reveals that the Se content in MPC-800/Se 50 is about 48.0 wt% (Figure SI-2). The two stages of weight loss in the TGA results, *i.e.* 350 °C–600 °C and 600 °C–900 °C, could be due to that Se was buried in micropores and mesopores with different sizes, which could result in different bonding energy between Se and C and thus different evaporation temperatures of Se in the TGA results. From the above results, it can be summarized that microporous carbon with high surface area and narrow pore distribution was successfully prepared by direct pyrolysis of PVDF powders, without any further activation process. The resulting MPC-800/Se 50 composite shows uniform distribution of Se in the microporous carbon.

3.1. Effect of PVDF carbonization temperature

In order to obtain the best electrochemical performance for MPC/Se

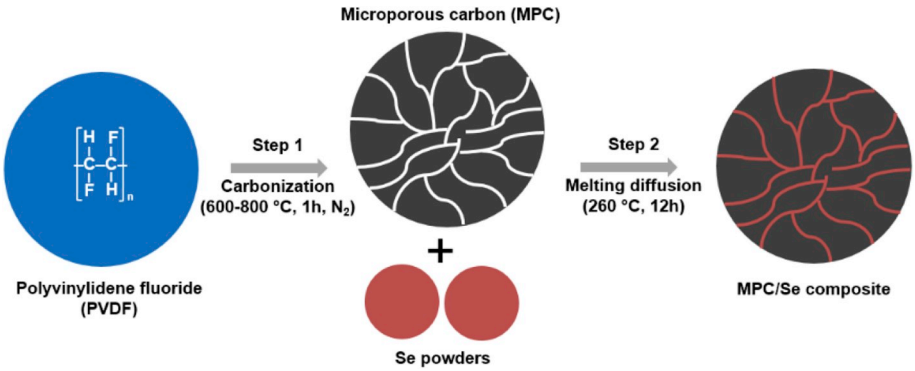

Fig. 1. Schematic illustration of the preparation process for microporous carbon (MPC) by the direct carbonization of PVDF at 600–800 °C for 1 h in N_2 atmosphere (Step 1), and for MPC/Se composites by melting diffusion of Se powders into MPC at 260 °C for 12 h (Step 2).

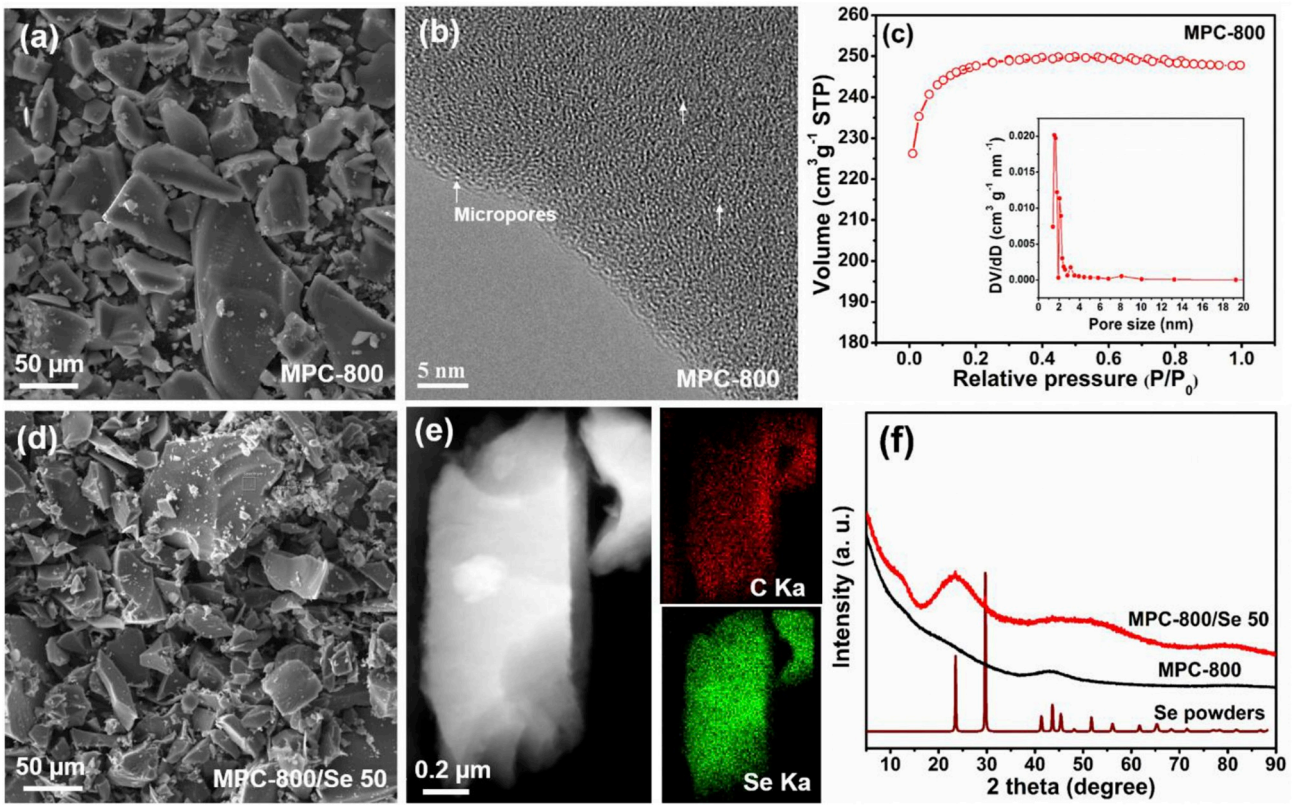

Fig. 2. (a) SEM image, (b) HRTEM image, and (c) BET isotherms and pore size distribution (inset) of MPC-800; (d) SEM image, (e) STEM image and EDS elemental mapping of C and Se, and (f) XRD patterns of MPC-800/Se 50, in comparison with MPC-800 and Se powders.

composites, systematic optimization was performed on MPC/Se cathodes, in terms of PVDF carbonization temperature, Se loading on the cathode, and Se content in MPC/Se. Fig. 3 presents the effects of PVDF carbonization temperature and Se loading on the performance of MPC/Se cathodes in Li-Se batteries. As seen in BET isotherms (Fig. 3a), all MPC carbonized at 600 °C, 700 °C, and 800 °C exhibit type-I isotherm, which is typical feature of "microporous solids" [28,29]. The main difference among these samples is the BET surface area, which is determined to be 731.2 $m^2 g^{-1}$, 671.3 $m^2 g^{-1}$, and 830.0 $m^2 g^{-1}$ for MPC-600, MPC-700, and MPC-800, respectively (Tables SI–1). Raman spectra of MPC-600, MPC-700 and MPC-800 show two broad distinct peaks at 1345 cm^{-1} and 1590 cm^{-1}, which are assigned to D band and G band, respectively [22,23,30]. The D band is due to disordered carbon originating from sp^3 carbons, whereas the G band is associated with a hexagonal carbon structure [22,23,30]. I_D/I_G ratios for all the samples are in a range of 2.4–2.6, suggesting similar degree of disorder in their carbon structure. Physical characterizations suggest that MPC obtained at different carbonization temperatures have no significant difference in their carbon structure, the type of pore size, and specific surface area.

Fig. 3c-f presents the electrochemical performance of MPC-600/Se 50, MPC-700/Se 50, and MPC-800/Se 50 cathode in Li-Se batteries based on 1 M $LiPF_6$ in EC:DEC carbonate electrolyte. As seen in Fig. 3c, all the cathodes exhibit a stable cycle stability over 100 cycles, and almost the same reversible capacity of 530 mAh g^{-1} at 0.1C. Discharge-charge curves of all the samples in the first cycle are featured with only one plateau at the same potential of 1.7 V–1.8 V, which suggests an one-step phase change between Se and Li_2Se ($Se + Li^+ + e^- \leftrightarrow Li_2Se$) and agrees well with previous work on Li-Se batteries based on carbonate electrolytes [15–24]. A one-step phase transition in charge-discharge profiles is one of the main characteristics of Li-Se batteries based on carbonate electrolytes, and suggests that Se is completely buried into the micropores of the carbon hosts [8,9,25,31]. This one-step reaction is further confirmed by CV curves (Figure SI-3), which show one pair of oxidation and reduction peaks located at ~ 1.2 V and 2.2 V, respectively. Coulombic efficiency (CE) in the first cycle is calculated to be 61.3%, 61.0%, and 59.1%, for MPC-600/Se 50, MPC-700/Se 50, and MPC-800/Se 50, respectively. In the following cycles, CE maintains over 99.6% for all the samples (Figure SI-4). The results in Fig. 3c-d reveal that although PVDF carbonization temperature affects specific surface area of MPC to some extent, it has inappreciable influence on the battery performance of MPC/Se composite cathodes. Since all MPC have mainly micropores in their structure (Fig. 3a), it can be concluded that micropores in the carbon plays a key role in enabling high specific capacity and excellent cyclic stability for MPC/Se composite cathodes. Long cycling stability of MPC-800/Se 50 is evaluated at 0.1C for 5 cycles and 0.5C for the following cycles, and presented in Fig. 3e. It can be seen that MPC-800/Se 50 exhibits a reversible capacity of ~400 mAh g^{-1} at 0.5C, and ultra-stable cyclic performance for 200 cycles, indicating the superior performance of MPC as a stable Se matrix. Furthermore, Se loading on the MPC/Se electrode (1.3–2 mg cm^{-2}) was controlled by adjusting the electrode thickness using a doctor blade, and the effect of Se loading on the specific capacity and areal capacity of MPC-800/Se 50 was investigated. As presented in Fig. 3f, the specific capacity of MPC-800/Se 50 gradually increases with the Se loading and reaches maximum 540 mAh g^{-1} with a Se loading of 1.6 mg cm^{-2}. Higher Se loadings result in a decrease in the specific capacity, probably due to electrolyte wetting issue in thick electrodes [27,32]. On the other hand, the specific areal capacity is elevated monotonously with the Se loading, and reach to 1.04 mAh cm^{-2} with a Se loading of 2.0 mg cm^{-2}.

The above results show that MPC derived from PVDF *via* an activation-free process is an excellent Se host material to enable stable, high capacity, and long-lifetime for Se cathode for Li-Se batteries in carbonate electrolytes. It should be noted that the mechanism of (de) lithiation of Se cathode in carbonate-based electrolytes is quite different from that in ether-based ones [8]. In ether-based electrolytes, Se undergoes multi-step phase transitions during the lithiation and

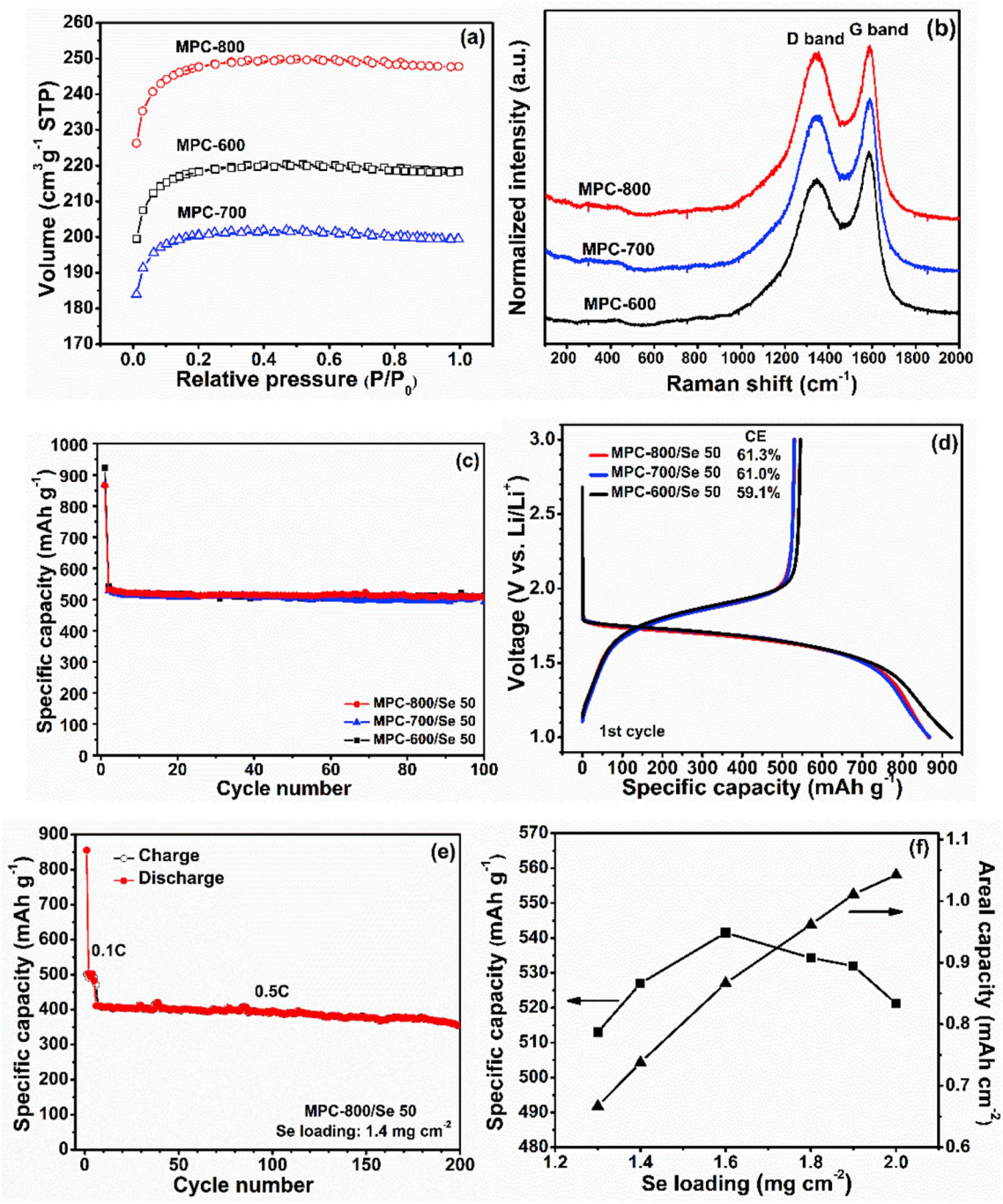

Fig. 3. (a) BET isotherms and (b) Raman spectra of MPC-600, MPC-700, and MPC-800; (c) cycling performance of MPC-600/Se 50, MPC-700/Se 50, and MPC-800/Se 50 with Se loadings of ~1.5 mg cm^{-2} at 0.1C; (d) 1st cycle charge and discharge curves for MPC-600/Se 50, MPC-700/Se 50, and MPC-800/Se 50; (e) long cycling stability of MPC-800/Se 50 measured at a current density of 0.1C in the first 5 cycles, and 0.5C in the following cycles; and (f) specific and areal capacities of MPC-800/Se 50 electrodes with Se loadings ranging from 1.3 to 2.0 mg cm^{-2} (specific and areal capacities are calculated using reversible discharge capacity in the 2nd cycle).

delithiation processes. During the lithiation process, Se will be first reduced to high-order polyselenides Se_n^{2-} ($n \geq 4$) and then further to Se_n^{2-} ($n \geq 4$) to Se_2^{2-} and Se^{2-} [8,9,13]. The soluble polyselenides in ether-based electrolytes can cause severe shuttle effect, leading to poor cycling life and low specific capacity of Se cathode [11,13]. In carbonate electrolytes, we observed only one plateau, suggesting only one phase transition during the lithiation and delithiation process for MPC-800/Se 50. The distinguished electrochemical performance in MPC-800/Se 50 could be attributed to the infiltration of Se into interior micropores of MPC, which can effectively confine Se to alleviate the dissolution of polyselenide and reduce the diffusion lengths for Li ions and electrons [15–22].

3.2. Effect of Se content in MPC/Se composites

Se content in MPC/Se composites is a critical factor that determines the overall energy density of Li-Se batteries at the system level. Therefore, the effect of Se contents (~50 wt%, 60 wt%, and 70 wt%) on electrochemical performance of MPC/Se cathodes was investigated by using the optimized MPC-800 as a model material.

N_2 adsorption-desorption isotherms analysis in Fig. 4a discloses that the BET surface area of MPC-800/Se 50, MPC-800/Se 60, and MPC-800/Se 70 significantly decreases to 18.2 $m^2 g^{-1}$, 3.0 $m^2 g^{-1}$, and 3.5 $m^2 g^{-1}$ respectively (Tables SI–1). This result suggests that the micropores in MPC-800 are completely filled for higher Se contents (MPC-800/Se 60 and MPC-800/Se 70), while a small portion of micropores remain unoccupied for MPC-800/Se 50. The XRD patterns in Fig. 4b reveals that strong and sharp diffraction peaks show up in MPC-800/Se 60 and MPC-800/Se 70, and could be assigned to trigonal Se. This is different from broad peaks for MPC-800/Se 50. The reason could be due to that for higher Se contents, Se will first completely fills the micopores of MPC-800, and then the remaining Se stays as "bulk type" on the outer surface of MPC particles. The bulk Se will contribute to the strong XRD diffraction peaks (Fig. 4b).

Electrochemical properties of MPC-800/Se 50, MPC-800/Se 60, and MPC-800/Se 70 in Li-Se batteries are compared in Fig. 4c-f. As shown in Fig. 4c, the 1st-cycle discharge capacity is 1088.5 mAh g^{-1}, 804.1 mAh g^{-1}, and 635.1 mAh g^{-1}, for MPC-800/Se 50, MPC-800/Se 60 and MPC-800/Se 70, respectively. The higher capacity than the theoretical value of Se (675 mAh g^{-1}) could be attributed to the decomposition of carbonate electrolytes and formation of SEI in the 1st cycle [16,19]. Moreover, difference between discharge and charge potentials becomes

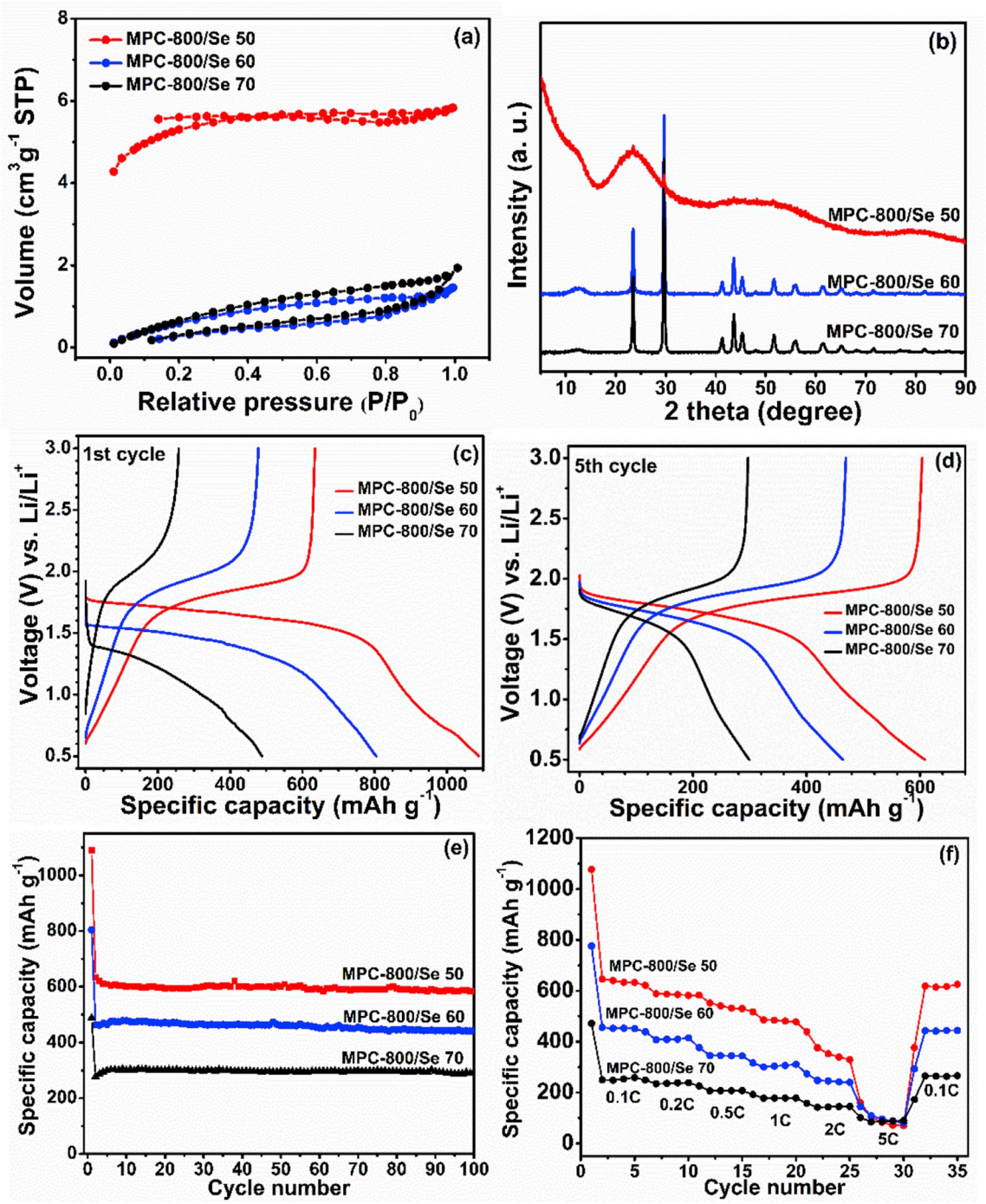

Fig. 4. (a) BET and (b) XRD patterns of MPC-800/Se 50, MPC-800/Se 60, and MPC-800/Se 70; charge-discharge curves in (c) the 1st cycle and (d) 5th cycle; (e) cycling performance at 0.1C and (f) rate capability of MPC-800/Se 50, MPC-800/Se 60, and MPC-800/Se 70 measured at different currents (0.1–5C) in a voltage range of 0.5–3 V.

significantly larger with the increased Se content from about ~50 wt% to 70 wt% in the MPC/Se composites, as shown in Fig. 4c and 4d for the 1st and the 5th cycle. Moreover, the CV analysis (Figure SI-3) reveals the broadening feature and larger separation between oxidation and reduction peaks with increasing Se contents, suggesting larger polarization and slower kinetics of electrochemical reactions for MPC/Se composites with higher Se contents. As a result, the lower cut-off voltage has to be extended from 1 V to 0.5 V for electrochemical testing of MPC-800/Se 50, MPC-800/Se 60, and MPC-800/Se 70, in order to complete the full lithiation reaction from Se to Li_2Se. As shown in Figure SI-5, MPC-800/Se 60 and MPC-800/Se 70 only deliver specific discharge capacities of 500 mAh g^{-1} and 350 mAh g^{-1}, respectively, in the 1st cycle in the voltage range of 1 V–3 V. This result shows that larger over-potential is required to initiate and complete the lithiation reaction for MPC/Se cathodes with higher Se contents. It is worth to note that a small plateau between 2 V and 1.5 V is observed in the 1st-cycle discharge curve of MPC-800/Se 60 and MPC-800/Se 70 (Figure SI-5), and is assigned to the dissolution of bulk Se into carbonate electrolytes in previous studies [15,18,19]. However, we did not observe the same phenomena in MPC-800/Se 50 (Fig. 4c). The cycling stability and rate capability of MPC-800/Se 50, MPC-800/Se 60, and MPC-800/Se 70 are shown in Fig. 4e and 4f, respectively. MPC-800/Se 50, MPC-800/Se 60, and MPC-800/Se 70 maintain reversible capacities of 583.4 mAh g^{-1}, 442.3 mAh g^{-1}, and 292.9 mAh g^{-1} over 100 cycles, with average CE over 99.5% from the 2nd to the 100th cycle (Figure SI-4). The rate capability measured at 0.1C–5C decreases in the order of MPC-800/Se 50 > MPC-800/Se 60 > MPC-800/Se 70 (Fig. 4f). For example, MPC-800/Se 50 could deliver a specific capacity of 350.3 mAh g^{-1} at 2C, while the reversible capacity is only 245.1 mAh g^{-1} and 150.1 mAh g^{-1} for MPC-800/Se 60 and MPC-800/Se 70, respectively. The charge-discharge profiles and XRD analysis (Fig. 4b and 4c, and Figure SI-4) strongly indicate that bulk Se exists in MPC-800/Se 60 and MPC-800/Se 70, but MPC-800/Se 50, and that the increasing Se content and unconfined Se (or bulk Se) result in the capacity loss for MPC-800/Se 60 and MPC-800/Se 70 [33].

In order to develop a better understanding on Se content effect on the electrochemical properties of MPC/Se composites, the CV curves for MPC-800/Se 50 and MPC-800/Se 70 are measured at various scan rates from 0.1 mV s^{-1} to 0.6 mV s^{-1} and showed in Fig. 5a and 5b. It can be found that the peak current is proportional to the square root of scan rates (Fig. 5c), indicating that the electrochemical reaction ($Se + Li^+ + e^- \leftrightarrow Li_2Se$) is diffusion-controlled [34,35]. The Li-ion diffusion coefficients (D_{Li}^+) are determined according to the Randles-Sevcik equation [34,35]:

$$I_p = 2.69 \times 10^5 n^{3/2} A D^{1/2} v^{1/2} C = B \times v^{1/2}$$

Where I_p is the peak current, n is the number of electrons involved in the reaction, A is the electrode area, C is the concentration of Li ions in the electrolyte, and B is the slope of the best-fit-curve in Fig. 5c. D_{Li}^+ is calculated to be 5.97×10^{-11} cm^2 s^{-1} (cathodic) and 5.84×10^{-11} cm^2 s^{-1} (anodic) for MPC-800/Se 50, and 5.29×10^{-12} cm^2 s^{-1} (cathodic) and 5.86×10^{-12} cm^2 s^{-1} (anodic) for MPC-800/Se 70. This result suggests that D_{Li}^+ in MPC/Se composite cathode is associated with the Se content, and higher Se content in MPC/Se composites leads to decrease in Li-ion diffusion rate, as schematically shown in Fig. 6. This explains the electrochemical performance difference among MPC-800/Se 50, MPC-800/Se 60, and MPC-800/Se 70 (Fig. 4). When micropore volume of carbon matrix is large enough to host all Se, Li ions from the electrolytes can quickly diffuse through SEI and react with Se (MPC 800/Se 50 in Fig. 6a). In contrast, when the Se content exceeds the maximum hosting capability of microporous carbon, the remaining Se will have to stay as bulk type on the outer surface of carbon, which will inevitably reduce Li-ion diffusion rate because of the large size of bulk Se (MPC 800/Se 70 in Fig. 6b). Therefore, bulk Se not only contributes little to reversible capacity, but also "disables" Se in micropores by blocking Li-ion diffusion channels, leading to significantly reduced capacity and rate capability in MPC/Se cathode with higher Se contents (Fig. 4e and 4f).

The above systematic study shows that micropores and micropore volume are the key merits for porous carbon as the Se host for Li-Se batteries based on carbonate electrolytes. Microporous carbon can effectively constrain Se in the space and prevent its dissolution into carbonate electrolytes during 1st discharge process, leading to highly reversible capacity and good cycling stability in Se cathodes [15–22]. In contrast, Se hosted in mesopores and macropores of the carbon or on the surface of carbon is generally irreversible, as evidenced by irreversible and higher discharge plateau in the 1st cycle in our work (Figure SI-5) and in others' results [15,18,19]. Therefore, it is the key to develop a porous carbon matrix with dominant microporous feature and high micropore volume in order to maximize Se content in the Se composite

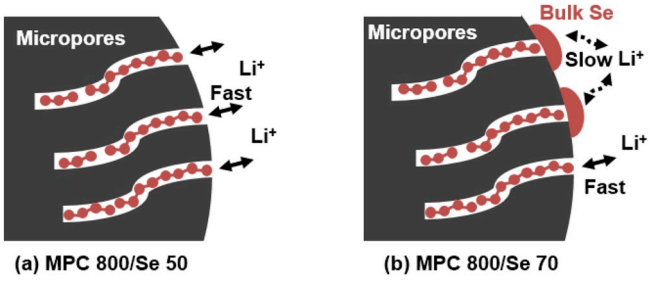

Fig. 6. Schematics of (a) MPC 800/Se 50 with all Se infiltrated into microspore carbon, allowing fast Li-ion diffusion from electrolytes to Se and (b) MPC 800/Se 70 with bulk Se distributed on the surface of carbon, which slows down diffusion of Li ions from/to Se in micropore carbon.

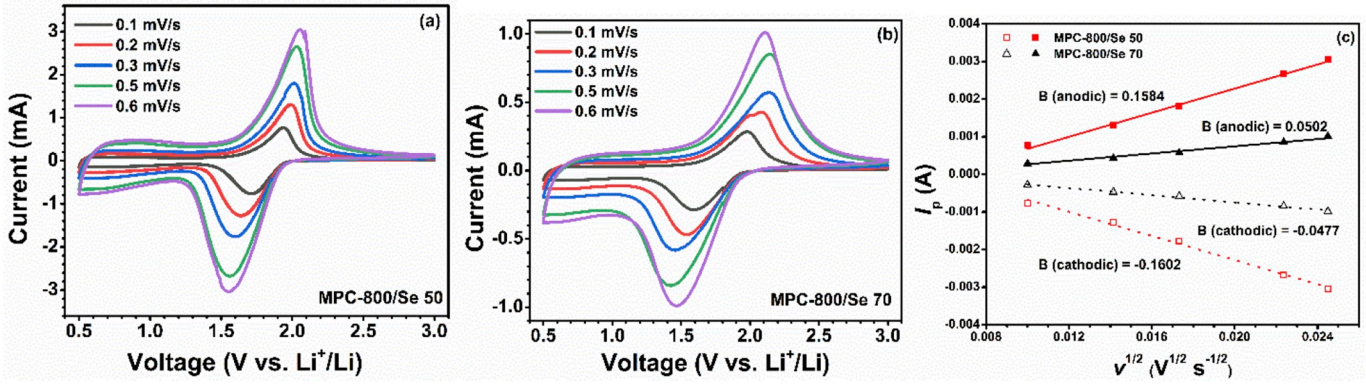

Fig. 5. CV curves of (a) MPC-800/Se 50 and (b) 50 MPC-800/Se 70 measured at 0.1. 0.2. 0.3. 0.5 and 0.6 mV s^{-1} between 0.5 V and 3.0 V; (c) linear fit of peak currents as a function of square root of scan rates obtained in (a) and (b).

cathodes. In order to reach 80 wt% of Se content in the Se composite, the micropore volume of the carbon matrix needs reach ~1.2 $cm^3 g^{-1}$ (Figure SI-6), which is still quite challenging and requires further process and material developments.

A detailed comparsion among this work and previous studies on Se cathode based in carbonate electrolyte is made, in terms of synthesis process, micropore volume, Se loading, Se content, and electrochemical performance (Tables SI–2). As a Se host material, MPC synthesized by one-step pyrolysis of commecial PVDF shows comparable electrochemical performance as nanostructued carbon fabricated through *via* sophicated and multil-step processes, such as ZIF-8 and MOF derived microporous carbon and CMK-3, *etc*. The simplicity of MPC synthesis process is an advantange for scaling up towards practical applications.

4. Conclusions

In summary, microporous carbon (MPC) with high surface area was successfully prepared by direct pyrolysis of PVDF in one step, and used as a host material for Se cathode in Li-Se batteries. The results suggested that micropores in MPC were the determinant factor for affecting the performance of MPC/Se composites. Carbonization temperatures for PVDF had negligible influence on the micropores and electrochemical performance of MPC/Se cathodes. Se contents in MPC/Se composites significantly affected the specific capacity and rate capability of MPC/Se cathodes. Increasing Se content from ~50 wt% to 70 wt% led to reduction of reversible capacity from 583.4 mAh g^{-1} to 292.9 mAh g^{-1} for MPC/Se cathode. The reason was attributed to bulk Se sitting outside of micropores, which resulted in reduced Li-ion diffusion coefficient in MPC/Se. The optimal MPC/Se cathode delivered a reversible capacity of 530 mAh g^{-1} at a current density of 0.1C, and exhibited an areal capacity up to 1.04 mA cm^{-1} with a Se loading of 2 mg cm^{-1}. The exceptional cyclability of MPC/Se cathodes was mainly due to the uniform distribution of Se in micropores, which could alleviate side reactions with electrolytes and prevent the dissolution of polyselenides in carbonate electrolytes.

Acknowledgements

This work was supported by Nature Sciences and Engineering Research Council of Canada (NSERC), Canada Foundation for Innovation (CFI), BC Knowledge Development Fund (BCKDF), and the University of British Columbia (UBC). The authors would like to thank Kristian David Mackowiak and Dr. Lukas Bichler in the School of Engineering at UBC for their kindly help on TG/DSC experiments. Special thanks to Dr. Carmen Andrei from Canadian Centre for Electron Microscopy (CCEM) at McMaster University for her assistance on HRTEM characterizations.

Appendix A. Supplementary data

Supplementary data to this article can be found online at https://doi.org/10.1016/j.jpowsour.2019.227059.

References

[1] J.-M. Tarascon, M. Armand, Issues and challenges facing rechargeable lithium batteries, ON Nat. 414 (2001) 359–367.
[2] X. Luo, J. Wang, M. Dooner, J. Clarke, Overview of current development in electrical energy storage technologies and the application potential in power system operation, Appl. Energy 137 (2015) 511–536.
[3] M.M. Thackeray, C. Wolverton, E.D. Isaacs, Electrical energy storage for transportation – approaching the limits of, and going beyond, lithium-ion batteries, Energy Environ. Sci. 5 (2012) 7854–7863.
[4] A. Manthiram, Y. Fu, S.H. Chung, C. Zu, Y.S. Su, Rechargeable lithium-sulfur batteries, Chem. Rev. 114 (2014) 11751–11787.
[5] X. Yang, X. Li, K. Adair, H. Zhang, X. Sun, Structural design of lithium–sulfur batteries: from fundamental research to practical application, Electrochem. Energy Rev. 1 (2018) 239–293.
[6] S.S. Zhang, Liquid electrolyte lithium/sulfur battery: fundamental chemistry, problems, and solutions, J. Power Sources 231 (2013) 153–162.
[7] D. Eroglu, K.R. Zavadil, K.G. Gallagher, Critical link between materials chemistry and cell-level design for high energy density and low cost lithium-sulfur transportation battery, J. Electrochem. Soc. 162 (2015) A982–A990.
[8] G.-L. Xu, J. Liu, R. Amine, Z. Chen, K. Amine, Selenium and selenium-sulfur chemistry for rechargeable lithium batteries: interplay of cathode structures, electrolytes, and interfaces, ACS Energy Lett 2 (2017) 605–614.
[9] C.-P. Yang, Y.-X. Yin, Y.-G. Guo, Elemental selenium for electrochemical energy storage, J. Phys. Chem. Lett. 6 (2015) 256–266.
[10] A. Abouimrane, D. Dambournet, K.W. Chapman, P.J. Chupas, W. Weng, K. Amine, A new class of lithium and sodium rechargeable batteries based on selenium and selenium–sulfur as a positive electrode, J. Am. Chem. Soc. 134 (2012) 4505–4508.
[11] D. Kundu, F. Krumeich, R. Nesper, Investigation of nano-fibrous selenium and its polypyrrole and graphene composite as cathode material for rechargeable Li-batteries, J. Power Sources 236 (2013) 112–117.
[12] R. Fang, G. Zhou, S. Pei, F. Li, H.-M. Cheng, Localized polyselenides in a graphene-coated polymer separator for high rate and ultralong life lithium–selenium batteries, Chem. Commun. 51 (2015) 3667–3670.
[13] X. Peng, L. Wang, X. Zhang, B. Gao, J. Fu, S. Xiao, K. Huo, P.K. Chu, Reduced graphene oxide encapsulated selenium nanoparticles for high-power lithium-selenium battery cathode, J. Power Sources 288 (2015) 214–220.
[14] Y. Cui, A. Abouimrane, C.-J. Sun, Y. Ren, K. Amine, Li–Se battery: absence of lithium polyselenides in carbonate based electrolyte, Chem. Commun. 50 (2014) 5576–5579.
[15] L. Zeng, W. Zeng, Y. Jiang, X. Wei, W. Li, C. Yang, Y. Zhu, Y. Yu, A flexible porous carbon nanofibers-selenium cathode with superior electrochemical performance for both Li-Se and Na-Se batteries, Adv. Energy Mater. 5 (2015) 1401377.
[16] J. Zhou, J. Yang, Z. Xu, T. Zhang, Z. Chen, J. Wang, A high performance lithium–selenium battery using a microporous carbon confined selenium cathode and a compatible electrolyte, J. Mater. Chem. 5 (2017) 9350–9357.
[17] Y. Liu, L. Si, X. Zhou, X. Liu, Y. Xu, J. Bao, Z. Dai, A selenium-confined microporous carbon cathode for ultrastable lithium–selenium batteries, J. Mater. Chem. 2 (2014) 17735–17739.
[18] Z. Li, L. Yin, MOF-derived, N-doped, hierarchically porous carbon sponges as immobilizers to confine selenium as cathodes for Li–Se batteries with superior storage capacity and perfect cycling stability, Nanoscale 7 (2015) 9597–9606.
[19] Y. Jiang, X. Ma, J. Feng, S. Xiong, Selenium in nitrogen-doped microporous carbon spheres for high-performance lithium–selenium batteries, J. Mater. Chem. A. 3 (2015) 4539–4546.
[20] Q. Cai, Y. Li, L. Wang, Q. Li, J. Xu, B. Gao, X. Zhang, K. Huo, P.K. Chu, Freestanding hollow double-shell Se@CN_x nanobelts as large-capacity and high-rate cathodes for Li-Se batteries, Nano Energy 32 (2017) 1–9.
[21] C. Luo, Y. Xu, Y. Zhu, Y. Liu, S. Zheng, Y. Liu, A. Langrock, C. Wang, Selenium@mesoporous carbon composite with superior lithium and sodium storage capacity, ACS Nano 7 (2013) 8003.
[22] C.-P. Yang, S. Xin, Y.-X. Yin, H. Ye, J. Zhang, Y.-G. Guo, An advanced selenium-carbon cathode for rechargeable lithium-selenium batteries, Angew. Chem. Int. Ed. 52 (2013) 8363–8367.
[23] Z. Li, L. Yuan, Z. Yi, Y. Liu, Y. Huang, Confined selenium within porous carbon nanospheres as cathode for advanced Li–Se batteries, Nano Energy 9 (2014) 229–236.
[24] H. Wang, S. Li, Z. Chen, H.K. Liu, Z. Guo, A novel type of one-dimensional organic selenium-containing fiber with superior performance for lithium–selenium and sodium–selenium batteries, RSC Adv. 4 (2014) 61673.
[25] J. Jin, X. Tian, N. Srikanth, L.B. Kong, K. Zhou, Advances and challenges of nanostructured electrodes for Li–Se batteries, J. Mater. Chem. 5 (2017) 10110–10126.
[26] H.J. Peng, J.Q. Huang, X.B. Cheng, Q. Zhang, Review on high-loading and high-energy lithium–sulfur batteries, Adv. Energy Mater. 7 (2017) 1700260.
[27] Z. Lin, T. Liu, X. Ai, C. Liang, Aligning academia and industry for unified battery performance metrics, Nat. Commun. 9 (2018) 5262.
[28] B. Xu, S. Hou, M. Chu, G. Cao, Y. Yang, Easy synthesis of a high surface area, hierarchical porous carbon for high-performance supercapacitors, Carbon 48 (2010) 2812.
[29] B. Xu, S. Hou, H. Duan, G. Cao, M. Chu, Y. Yang, Ultramicroporous carbon as electrode material for supercapacitors, J. Power Sources 228 (2013) 193.
[30] J. Liu, Y. Zhang, M.I. Ionescu, R. Li, X. Sun, Nitrogen-doped carbon nanotubes with tunable structure and high yield produced by ultrasonic spray pyrolysis, Appl. Surf. Sci. 257 (2011) 7837–7844.
[31] A. Eftekhari, The rise of lithium–selenium batteries, Sustain. Energ. Fuels 1 (2017) 14.
[32] D. Lv, J. Zheng, Q. Li, X. Xie, S. Ferrara, Z. Nie, L.B. Nehdi, N.D. Browning, J. G. Zhang, J. Liu, J. Xiao, High energy density lithium–sulfur batteries: challenges of thick sulfur cathodes, Adv. Energy Mater. 5 (2015) 1402290.
[33] X. Peng, L. Wang, X. Zhang, B. Gao, J. Fu, S. Xiao, K. Huo, P.K. Chu, Reduced graphene oxide encapsulated selenium nanoparticles for high-power lithium-selenium battery cathode, J. Power Sources 288 (2015) 214–220.
[34] J. Zhou, Y. Guo, C. Liang, J. Yang, J. Wang, Y. Nuli, Confining small sulfur molecules in peanut shell-derived microporous graphitic carbon for advanced lithium sulfur battery, Electrochim. Acta 273 (2018) 127–135.
[35] M. Park, X. Zhang, M. Chung, G.B. Less, A.M. Sastry, A review of conduction phenomena in Li-ion batteries, J. Power Sources 195 (2010) 7904–7929.